The $\rho\rho$ interaction in the hidden gauge formalism and the $f_0(1370)$ and $f_2(1270)$ resonances.

R. Molina[1], D. Nicmorus[2] and E. Oset[1]

November 28, 2008

[1] Departamento de Física Teórica and IFIC, Centro Mixto Universidad de Valencia-CSIC, Institutos de Investigación de Paterna, Aptdo. 22085, 46071 Valencia, Spain
[2] Fachbereich Theoretische Physik, Institut für Physik,Karl-Franzens-Universität Graz, Universitätsplatz 5, A-8010 Graz, Austria

Abstract

We have studied the interaction of vectors mesons within the hidden gauge formalism and applied it to the particular case of the $\rho\rho$ interaction. We find a strong attraction in the isospin, spin channels I,S=0,0 and 0,2, which is enough to bind the $\rho\rho$ system. We also find that the attraction in the I,S=0,2 channel is much stronger than in the 0,0 case. The states develop a width when the ρ mass distribution is considered, and particularly when the $\pi\pi$ decay channel is turned on. Using a regularization scheme with cut offs of natural size, we obtain results in fair agreement with the mass and the width of the $f_0(1370)$ and $f_2(1270)$ meson states, providing a natural explanation of why the tensor state is more bound than the scalar and offering a new picture for these states, which would be dynamically generated from the $\rho\rho$ interaction or, in simpler words, $\rho\rho$ molecular states.

1 Introduction

Chiral perturbation theory, with its unitary extensions to higher energies has brought a new momentum to hadron physics at low and intermediate energies. The exact unitarity in coupled channels together with dispersion relations [1, 2], the inverse amplitude method (IAM) [3, 4] or the equivalent solution in terms of coupled Bethe Salpeter equations [5, 6, 7] introduce a nonperturbative scheme that proves highly efficient to study meson-meson or meson-baryon interactions, usually referred to as the chiral unitary approach. By fixing a minimum of subtraction constants or cut offs to regularize the loops, one finds a fair agreement with data in a vast amount of reactions [8] (see [9] for a recent review). One of the results of these studies is that the amplitudes have sometimes poles that can be associated to known resonances. Sometimes new

resonances are predicted, like a second $\Lambda(1405)$ [10] or a second $K_1(1270)$ axial vector meson [11], for which experimental support has been found in [12] and [13] respectively. So far, resonances have been investigated in the interaction of the SU(3) octet of the pseudoscalar mesons of the π with themselves [6, 7, 14, 3, 4], which provide the low lying scalar mesons, the interaction of the pseudoscalar mesons with the octet of baryons of the p, which generate $J^P = 1/2^-$ baryonic resonances [5, 15, 2, 16, 10, 17, 18], the interaction of pseudoscalar mesons with the decuplet of the Δ [19, 20], which leads to $J^P = 3/2^-$ baryon resonances, and the interaction of pseudoscalar mesons with vector mesons, which leads to axial vector meson resonances [21, 11]. Yet, the interaction of vector mesons with themselves has not been tackled from this perspective. The purpose of the present paper is to study this interaction and show how, also in this case, one obtains dynamically generated resonances.

The interaction of vector mesons with themselves is done using the Lagrangians of hidden gauge formalism, which mix vector mesons with pseudoscalars and respect chiral symmetry [22, 23]. The hidden gauge Lagrangians for vector-vector interaction do not provide local chiral Lagrangians as in the case of meson-meson or meson-baryon interaction discussed above. Non local terms corresponding to the exchange of vector mesons appear in the amplitudes. Yet, under certain approximations these terms can also be recast in the form of local Lagrangians similar to those quoted above. In this first paper on the issue we shall describe the formalism and apply it to study the $\rho - \rho$ interaction. We shall see that one gets attraction in the $I = 0, S = 0$ and $I = 0, S = 2$ channels which is enough to produce bound states of $\rho - \rho$. We shall see that the interaction in the $I = 0, S = 2$ tensor case is stronger than in the scalar one $I = 0, S = 0$ and that the states that we obtain can be associated to the known resonances $f_0(1370)$ and $f_2(1270)$. In order to obtain the width of the states we shall also consider their decay into $\pi\pi$, obtained within the same formalism of [22, 23].

On the theoretical side there is work done for both resonances. The coupling of the tensor resonance to $\pi\pi$ was exploited in [24], within the formalism of the IAM, and the $f_2(1270)$ was obtained qualitatively, at the expense of adding counterterms or higher order that produce the resonance within this formalism. This does not mean that the $f_2(1270)$ is a resonance built up from $\pi\pi$. The information on the resonance properties is essentially buried in the counterterms, like in the case of the ρ meson that is also obtained within the IAM [3, 4] starting from the $\pi\pi$ interaction. There again, the basic properties of the rho are tied to the L_i coefficients of the second order chiral Lagrangian [31], and its generation within the IAM does not mean that one has a dynamically generated resonance from the basic $\pi\pi$ interaction. Indeed, a careful study of the large N_c behavior of the resonance shows that the state remains as N_c goes to infinite, as corresponds to genuine states that are built essentially from $q\bar{q}$, unlike the dynamically generated scalar mesons that fade away in that limit [32]. In the present case the counterterms needed in the IAM to produce this state in [24] are burying the information about the nature of the $f_2(1270)$ resonance, which, as we will show, gets dynamically generated from the $\rho\rho$ interaction. Work with quark models is also available. In [25] the $f_0(1370)$ is assumed to be dominantly a $q\bar{q}$ state, unlike the lighter scalars that are assumed to be largely four quark states. In [26] the $f_0(1370)$ is also studied within the improved ladder approximation of QCD assuming it to be mostly made of $q\bar{q}$ components, although, as quoted there, the meson-meson or four quark components are supposed to be important. In [27] the $f_0(1370)$ is assumed to be a mixture of $q\bar{q}$ and four quarks, while in [28] a mixture of $q\bar{q}$ components with glueballs is preferred. Once again, in [29] the $q\bar{q}$ nature is preferred for the $f_0(1370)$ with the quarks of non strange nature. For the case of the

$f_2(1270)$ there is also work done in [30], where the state is assumed to be predominantly a $q\bar{q}$ state.

Our work will bring a new perspective into this panorama, showing that practically with no freedom (up to fine tuning of a cut off parameter from values around the natural size), the $f_2(1270)$ and $f_0(1370)$ states emerge as bound states of the $\rho\rho$ interaction evaluated within the reliable formalism of hidden gauge.

2 Formalism for VV interaction

We follow the formalism of the hidden gauge interaction for vector mesons of [22, 23](see also [33] for a practical set of Feynman rules). The interaction Lagrangian involving the interaction of vector mesons amongst themselves is given by

$$\mathcal{L}_{III} = -\frac{1}{4}\langle V_{\mu\nu}V^{\mu\nu}\rangle \ , \tag{1}$$

where the symbol $\langle\rangle$ stands for the trace in the $SU(3)$ space and $V_{\mu\nu}$ is given by

$$V_{\mu\nu} = \partial_\mu V_\nu - \partial_\nu V_\mu - ig[V_\mu, V_\nu] \ , \tag{2}$$

with g given by

$$g = \frac{M_V}{2f} \ , \tag{3}$$

with $f = 93\,MeV$ the pion decay constant. The value of g of eq. (3) is one of the ways to account for the $KSFR$ rule [34], which is tied to vector meson dominance [35]. The magnitude V_μ is the $SU(3)$ matrix of the vectors of the octet of the ρ

$$V_\mu = \begin{pmatrix} \frac{\rho^0}{\sqrt{2}} + \frac{\omega}{\sqrt{2}} & \rho^+ & K^{*+} \\ \rho^- & -\frac{\rho^0}{\sqrt{2}} + \frac{\omega}{\sqrt{2}} & K^{*0} \\ K^{*-} & \bar{K}^{*0} & \phi \end{pmatrix}_\mu \ . \tag{4}$$

The interaction of $\mathcal{L}_{III}$ gives rise to a contact term coming for $[V_\mu, V_\nu][V_\mu, V_\nu]$

$$\mathcal{L}_{III}^{(c)} = \frac{g^2}{2}\langle V_\mu V_\nu V^\mu V^\nu - V_\nu V_\mu V^\mu V^\nu\rangle \ , \tag{5}$$

depicted in fig. 1 a), and on the other hand it gives rise to a three vector vertex

$$\mathcal{L}_{III}^{(3V)} = ig\langle(\partial_\mu V_\nu - \partial_\nu V_\mu)V^\mu V^\nu\rangle \ , \tag{6}$$

depicted in fig. 1 b). This latter Lagrangian gives rise to a $VV \to VV$ interaction by means of the exchange of one of the vectors, as shown in fig. 1 c). These Lagrangians have been previously used to study collision rates of vector mesons in heavy ion collisions [36].

The $SU(3)$ structure of the Lagrangian allows us to take into account all the channels within $SU(3)$ which couple to certain quantum numbers. This is what is done in the study of the interaction of pseudoscalar mesons [6, 7] where, for instance, for the scalar-isoscalar channel one introduces the $\pi\pi$ and $K\bar{K}$ pairs as coupled channels. In this particular case the interaction
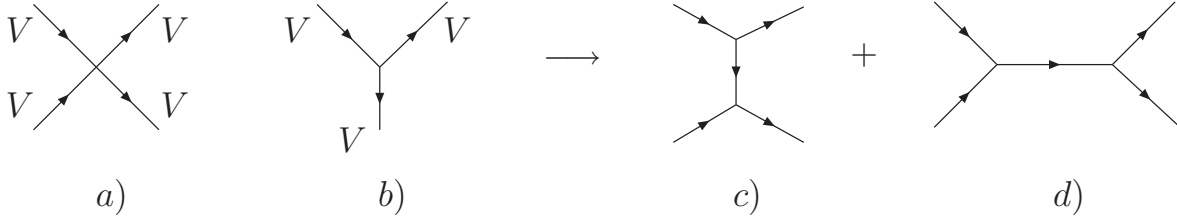
3

Figure 1: Terms of the $\mathcal{L}_{III}$ Lagrangian: a) four vector contact term, eq. (5); b) three vector interaction, eq. (6); c) t and u channels from vector exchange; d) s channel for vector exchange.
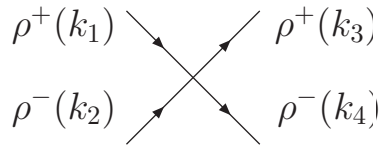

Figure 2: Contact term of the $\rho\rho$ interaction.

leads to the generation of two scalar isoscalar resonances, the $f_0(600)$ or σ and the $f_0(980)$. It is also seen that the $\pi\pi$ and $K\bar{K}$ states largely decouple: the σ is basically $\pi\pi$ resonance, while the $f_0(980)$ couples mostly to $K\bar{K}$ and weakly to $\pi\pi$, as a consequence of which one has a small width for the $f_0(980)$ in spite of the large phase space for decay into $\pi\pi$.

In the present work we shall provide the formalism for the VV interaction and present results for the simplest case, the $\rho\rho$ interaction. We are aiming at obtaining from this interaction the lightest scalar and tensor mesons after the $f_0(980)$ which is very well reproduced in terms of pseudoscalar-pseudoscalar components. In the PDG [37] we find the $f_2(1270)$ and the $f_0(1370)$. The $\rho\rho$ system interacting in S wave, as we shall do, can lead to different isospin, spin states $I, J = 0, 0; 1, 1; 0, 2; 2, 0$ and $2, 2$. It would be most interesting to see if the results that we obtain agree, at least qualitatively, with the experimental data on this sector at low energies. In particular, it is challenging to find a reason on why the $f_2(1270)$ is lower in energy than the $f_0(1370)$. In this exploratory work we shall work only with ρ meson, with the limited aim to learn about the structure of these low lying resonances. The use of couple channels is welcome and should be tackled in the future, but for purpose of studying these low lying resonances, the other channel, $K^*\bar{K}^*$, has a mass of $1784\,MeV$, more than $400\,MeV$ higher than the mass of the $f_0(1370)$, and then, as is the case in all studies of meson-meson interaction, this channel can barely affect the structure of these low lying resonances. In any case, its possible effect, through a weakly energy dependent $K\bar{K}$ loop function at the energies that we are concerned, can be accommodated by fine tuning the subtraction constants of the regularized $\rho\rho$ loop function, or equivalently the cut off, as we shall do.

Starting with the Lagrangian of eq. (5) we can immediately obtain the corresponding amplitude to $\rho^+\rho^- \to \rho^+\rho^-$ corresponding to fig. 2.

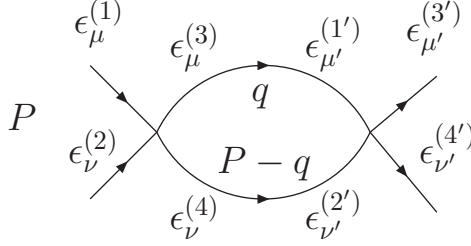Figure 3: Loop function for two mesons.

We immediately obtain[1]:

$$-it^{(c)}_{\rho^+\rho^-\to\rho^+\rho^-} = i2g^2(2\epsilon_\mu^{(1)}\epsilon_\nu^{(2)}\epsilon_\nu^{(3)}\epsilon_\mu^{(4)} - \epsilon_\mu^{(1)}\epsilon_\mu^{(2)}\epsilon_\nu^{(3)}\epsilon_\nu^{(4)} - \epsilon_\mu^{(1)}\epsilon_\nu^{(2)}\epsilon_\mu^{(3)}\epsilon_\nu^{(4)}) \ , \tag{7}$$

where the indices $1, 2, 3$ and 4 correspond to the particles with momenta k_1, k_2, k_3 and k_4 in fig. 2. For simplicity of the notation we write the Lorentz indices as subindices with the understanding that repeated indices should be one covariant and the other one contravariant.

Eq. (7) shows three different structures of the vector polarizations, the same number as possible spins of the two ρ systems, and there is some relationship as we shall see below.

The large mass of the vectors offers a technical advantage, since the three momenta of the ρ in the scattering amplitude in the region of energies of interest to us are small compared to its mass. We shall work in the limit of small three momenta of the ρ where the ϵ_μ components are only nonvanishing for the spatial indices, this is, we take $\epsilon_0 \equiv 0$ for practical purposes (recall $\epsilon^0(linear\ polarization) = \frac{k}{M_V}$ and $\epsilon^0 = 0$ for the two transverse polarizations).

3   Spin projectors

Next we want to find the appropriate projectors in $S = 0, 1, 2$ in terms of the different combinations of the four polarization vectors. For this purpose we look into the loop diagram of fig. 3, where the interaction has been iterated to provide the second term of the Bethe Salpeter equation. Take the term $\epsilon_\mu^{(1)}\epsilon_\nu^{(2)}\epsilon_\mu^{(3)}\epsilon_\nu^{(4)}$ and iterate it. We get the structure

$$\epsilon_\mu^{(1)}\epsilon_\nu^{(2)}\epsilon_\mu^{(3)}\epsilon_\nu^{(4)}\epsilon_{\mu'}^{(1')}\epsilon_{\nu'}^{(2')}\epsilon_{\mu'}^{(3')}\epsilon_{\nu'}^{(4')} \ , \tag{8}$$

with the contraction of the internal indices $3, 1'$ and $4, 2'$ leading, after summing over the possible polarizations, to

$$(-g_{\mu\mu'} + \frac{q_\mu q_{\mu'}}{M_V^2})(-g_{\nu\nu'} + \frac{(P-q)_\nu(P-q)_{\nu'}}{M_V^2}) \ , \tag{9}$$

where P is the total momentum of the $\rho\rho$ system. Since μ, ν, μ', ν' are all external indices, all of them are spatial and the sum above reverts into $(i, j = 1, 2, 3)$

$$(\delta_{ii'} + \frac{q_i q_{i'}}{M_V^2})(\delta_{jj'} + \frac{q_j q_{j'}}{M_V^2}) \ . \tag{10}$$

---

[1]We always use a carthesian basis for the polarization vectors. Should one use a spherical basis, one should complex conjugate the ϵ_μ of the outgoing vectors.
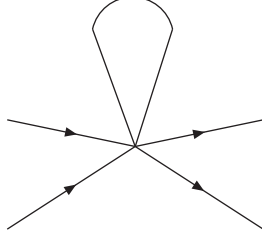
Figure 4: Topology of the part of the diagram of fig. 3 coming from off-shell parts of the polarization sums.

We shall work in a renormalization scheme which relies upon the function of q apart from the two propagators in the loop function, $f(q)$, being evaluated on shell. The base for it can be seen in the N/D method [1, 2] which relies upon the potential and the T-matrix factorized on shell in the loops as a result of the use of a dispersion relation on T^{-1} after imposing unitarity. Another method of work is to recast $f(q)$ as $f(q_{on-shell}) + (f(q) - f(q_{on-shell}))$. Obviously $f(q) - f(q_{on-shell})$ vanishes for $q = q_{on-shell}$, as a consequence of which it cancels the singularity of one meson propagator and one gets a diagram with a topology as in fig. 4 (the argument is the same when dealing with the off shell part of the other meson). This diagram gets canceled by tadpoles in the calculation or otherwise can be argued to renormalize the lowest order of the $\rho\rho \to \rho\rho$ potential.

The arguments above imply that we take $q_i, q_{i'}$ on shell in eq. (10) and $\frac{q_i q_{i'}}{M_V^2}$ is negligible and we ignore it. The argument used above is slightly different for the structure $\epsilon_\mu^{(1)} \epsilon_\mu^{(2)} \epsilon_\nu^{(3)} \epsilon_\nu^{(4)}$. Indeed, now we have the combination

$$\epsilon_\mu^{(1)} \epsilon_\mu^{(2)} \epsilon_\nu^{(3)} \epsilon_\nu^{(4)} \epsilon_{\mu'}^{(1')} \epsilon_{\mu'}^{(2')} \epsilon_{\nu'}^{(3')} \epsilon_{\nu'}^{(4')} \; , \tag{11}$$

and contract the indices of $3, 1'$ and $4, 2'$ summing over polarizations such that we get

$$(-g_{\nu\mu'} + \frac{q_\nu q_{\mu'}}{M_V^2})(-g_{\nu\mu'} + \frac{(P-q)_\nu (P-q)_{\mu'}}{M_V^2}) \; . \tag{12}$$

The fact that the external indices μ, ν' are spatial does not tell us anything on the internal indices ν, μ' which can also be time like. We can distinguish three cases:

i) $\nu = i, \mu' = j'$ space like. On shell we get $\delta_{ij'}\delta_{ij'}$ with correction of $O(\vec{q}^2/M_V^2)$ that we neglect.

ii) $\nu = 0, \mu' = i$ or vice versa. We get non vanishing terms from $q^0(P-q)^0\vec{q}^2/M_V^4$ which are again of the order of $\vec{q}^2/M_V^2$. The whole term is neglected.

iii) $\nu = 0, \mu' = 0$. Now the term

$$(-g_{00} + \frac{q_0 q_0}{M_V^2})(-g_{00} + \frac{(P-q)_0 (P-q)_0}{M_V^2}) \; , \tag{13}$$

vanishes on shell up to terms of $\vec{q}^2/M_V^2$, which we again neglect.

6

The discussion has served to show that the regularization procedure is slightly different for different combinations of the polarization vectors, and hence, for the different spin terms. This implies that in dimensional regularization one cannot invoke exactly the same substraction constant in all channels but they cannot be too different either. We use cut off renormalization, and the former findings would imply possible different cut offs in different channels but not too different, and they must be of natural size. We show results in the present paper for different possible cut offs of natural size. There is another reason to allow for some freedom in the subtraction constants for different spins, since we make the approximation $\frac{q^2}{M_V^2} = 0$ in the exchanged vectors. Given the large width of the ρ meson, a consideration of the ρ mass convolution for the four ρ mesons in the amplitudes has a consequence that this quantity would not be fully negligible for some distribution of masses in the convolution. We have evaluated the average value of $\frac{q^2}{M_V^2}$ for forward scattering with the convolution of the four $\rho's$ and find q^2/M_V^2 of the order of $10\,\%$, enough to justify our calculations, but inside loops this quantity can be bigger and it is also $s-$dependent. Once again, these effects could be accounted for by means of fine tunning of the substraction constants mentioned before for different channels.

For practical purposes, in this renormalization scheme we only need the transverse components in all cases, and in the propagators of the vector mesons we can take

$$\langle T\left[\rho_i \rho_{i'}\right]\rangle = \frac{\delta_{ii'}}{q^2 - M_V^2 + i\epsilon} \tag{14}$$

or the same expression with $q \to P - q$ for the second propagator.

After this exercise it is easy to check that the three independent structures that upon iteration lead to the same structure are given by

$$
\begin{aligned}
\mathcal{P}^{(0)} &= \frac{1}{3}\epsilon_i^{(1)}\epsilon_i^{(2)}\epsilon_j^{(3)}\epsilon_j^{(4)} \\
\mathcal{P}^{(1)} &= \frac{1}{2}(\epsilon_i^{(1)}\epsilon_j^{(2)} - \epsilon_j^{(1)}\epsilon_i^{(2)})\frac{1}{2}(\epsilon_i^{(3)}\epsilon_j^{(4)} - \epsilon_j^{(3)}\epsilon_i^{(4)}) \\
\mathcal{P}^{(2)} &= \{\frac{1}{2}(\epsilon_i^{(1)}\epsilon_j^{(2)} + \epsilon_j^{(1)}\epsilon_i^{(2)}) - \frac{1}{3}\epsilon_l^{(1)}\epsilon_l^{(2)}\delta_{ij}\} \\
&\times \quad \{\frac{1}{2}(\epsilon_i^{(3)}\epsilon_j^{(4)} + \epsilon_j^{(3)}\epsilon_i^{(4)}) - \frac{1}{3}\epsilon_m^{(3)}\epsilon_m^{(4)}\delta_{ij}\} \ .
\end{aligned}
\tag{15}
$$

It is also easy to see that these structures project over the three different states of spin, $S = 0, 1, 2$ respectively, by taking states with a certain third component of the spin and writing them in terms of spherical vectors $\mp\frac{1}{\sqrt{2}}(\epsilon_1 \pm i\epsilon_2)$ and ϵ_3.

Although we have to keep in mind that we will be dealing with spatial components, it is convenient to write these projectors in covariant form such as to easily separate the structures that appear from the Lagrangians into the different spin projectors. So we write

$$
\begin{aligned}
\mathcal{P}^{(0)} &= \frac{1}{3}\epsilon_\mu \epsilon^\mu \epsilon_\nu \epsilon^\nu \\
\mathcal{P}^{(1)} &= \frac{1}{2}(\epsilon_\mu \epsilon_\nu \epsilon^\mu \epsilon^\nu - \epsilon_\mu \epsilon_\nu \epsilon^\nu \epsilon^\mu) \\
\mathcal{P}^{(2)} &= \{\frac{1}{2}(\epsilon_\mu \epsilon_\nu \epsilon^\mu \epsilon^\nu + \epsilon_\mu \epsilon_\nu \epsilon^\nu \epsilon^\mu) - \frac{1}{3}\epsilon_\alpha \epsilon^\alpha \epsilon_\beta \epsilon^\beta\} \ ,
\end{aligned}
\tag{16}
$$

7

where the order $1, 2, 3, 4$ in the polarization vectors is understood (this allows us to write the expressions covariantly without complication in the indices. We use the covariant formalism in what follows).

4   Isospin projection

We must now evaluate the amplitudes for the isospin states:

$$
\begin{aligned}
|\rho\rho, I = 0\rangle &= -\frac{1}{\sqrt{6}}|\rho^+(k_1\epsilon_1)\rho^-(k_2\epsilon_2) + \rho^-(k_1\epsilon_1)\rho^+(k_2\epsilon_2) + \rho^0(k_1\epsilon_1)\rho^0(k_2\epsilon_2)\rangle \\
|\rho\rho, I = 1, I_3 = 0\rangle &= -\frac{1}{2}|\rho^+(k_1\epsilon_1)\rho^-(k_2\epsilon_2) - \rho^-(k_1\epsilon_1)\rho^+(k_2\epsilon_2)\rangle \\
|\rho\rho, I = 2, I_3 = 0\rangle &= -\frac{1}{\sqrt{2}}|\frac{1}{\sqrt{6}}(\rho^+(k_1\epsilon_1)\rho^-(k_2\epsilon_2) + \rho^-(k_1\epsilon_1)\rho^+(k_2\epsilon_2)) \\
&\quad -\sqrt{\frac{2}{3}}\rho^0(k_1\epsilon_1)\rho^0(k_2\epsilon_2)\rangle
\end{aligned}
\tag{17}
$$

Note that we are using the unitary normalization [6], with an extra factor $\frac{1}{\sqrt{2}}$ such that when summing over intermediate states of identical particles we obtain the resolution of the identity, i.e. $\frac{1}{2}\sum_q |\rho^0(\vec{q})\rho^0(-\vec{q})\rangle\langle\rho^0(\vec{q})\rho^0(-\vec{q})| = 1$. One must correct the final amplitudes for the "wrong" normalization on the external legs, with a global normalization factor that does not affect the search for the poles or the energy dependence of the amplitudes. We also take the phase convention $|\rho^+\rangle = -|1, 1\rangle$ of isospin.

By using the isospin wave functions and the Lagrangian of eq. (5) we obtain for $I = 1$

$$
t^{(I=1)} = 3g^2(\epsilon_\mu\epsilon_\nu\epsilon^\mu\epsilon^\nu - \epsilon_\mu\epsilon_\nu\epsilon^\nu\epsilon^\mu) ,
\tag{18}
$$

which according to the spin projection operators of eq. (16) only has the $S = 1$ component, consistent with the rule $L + S + I = even$. Thus we have

$$
t^{(I=1,S=1)} \equiv 6g^2 .
\tag{19}
$$

The interaction is repulsive, however we still have to evaluate the contribution from the vector exchange mechanisms. In $I = 0$ we get the amplitude

$$
t^{(I=0)} = 2g^2\{2\epsilon_\mu\epsilon^\mu\epsilon_\nu\epsilon^\nu - \epsilon_\mu\epsilon_\nu\epsilon^\mu\epsilon^\nu - \epsilon_\mu\epsilon_\nu\epsilon^\nu\epsilon^\mu\} ,
\tag{20}
$$

which by means of the spin projection structures leads to

$$
\begin{aligned}
t^{(I=0,S=0)} &= 8g^2 \\
t^{(I=0,S=2)} &= -4g^2 .
\end{aligned}
\tag{21}
$$

We can see that the interaction in the $I = 0, S = 0$ channel is repulsive but the one in $S = 2$ is attractive. We still need, however, the contribution of the vector exchange terms. Note again that according to the rule $L + S + I = even$ we do not get contribution of $S = 1$ for $I = 0$. In $I = 2$ we obtain the amplitude

$$
t^{(I=2)} = -g^2(2\epsilon_\mu\epsilon^\mu\epsilon_\nu\epsilon^\nu - \epsilon_\mu\epsilon_\nu\epsilon^\mu\epsilon^\nu - \epsilon_\mu\epsilon_\nu\epsilon^\nu\epsilon^\mu) ,
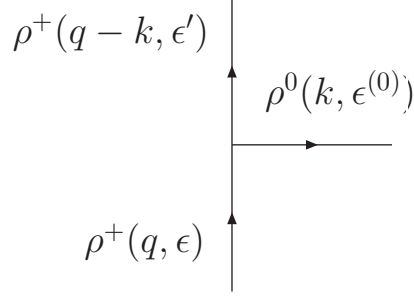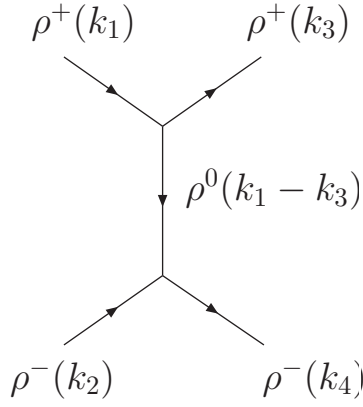\tag{22}
$$

Figure 5: Three vector vertex diagram.

Figure 6: Vector exchange diagram for $\rho^+ \rho^- \to \rho^+ \rho^-$.

which projected over spin states leads to

$$
\begin{aligned}
t^{(I=2,S=0)} &= -4g^2 \\
t^{(I=2,S=2)} &= 2g^2 \ .
\end{aligned}
\tag{23}
$$

5 Vector exchange terms

From the Lagrangian of eq.(6) we get the three vector vertex depicted in fig. 5. The vertex function corresponding to the diagram of fig. 3 is given by

$$
\begin{aligned}
-it^{(3)} = \ -\ &\sqrt{2}g\{(ik_\mu\epsilon^{(0)}_\nu - ik_\nu\epsilon^{(0)}_\mu)\epsilon^\mu\epsilon'^\nu \\
+\ &(-iq_\mu\epsilon_\nu + iq_\nu\epsilon_\mu)\epsilon'^\mu\epsilon^{(0)\nu} \\
+\ &(i(q-k)_\mu\epsilon'_\nu - i(q-k)_\nu\epsilon'_\mu)\epsilon^{(0)\mu}\epsilon^\nu\} \ ,
\end{aligned}
\tag{24}
$$

with this basic structure we can readily evaluate the amplitude of the diagram of fig. 6 and we obtain

$$
\begin{aligned}
- it^{(ex)} = \ & - \ \sqrt{2}g\{(i(k_1 - k_3)_\mu \epsilon_\nu^{(0)} - i(k_1 - k_3)_\nu \epsilon_\mu^{(0)})\epsilon^{(1)\mu}\epsilon^{(3)\nu} \\
& + \ (-ik_{1\mu}\epsilon_\nu^{(1)} + ik_{1\nu}\epsilon_\mu^{(1)})\epsilon^{(3)\mu}\epsilon^{(0)\nu} + (ik_{3\mu}\epsilon_\nu^{(3)} - ik_{3\nu}\epsilon_\mu^{(3)})\epsilon^{(0)\mu}\epsilon^{(1)\nu}\} \\
& \times \ \frac{i}{(k_1 - k_3)^2 - M_\rho^2 + i\epsilon} \\
& \times \ (-\sqrt{2})g\{(-i(k_2 - k_4)_{\mu'}\epsilon_{\nu'}^{(0)} + i(k_2 - k_4)_{\nu'}\epsilon_{\mu'}^{(0)})\epsilon^{(4)\mu'}\epsilon^{(2)\nu'} \\
& + \ (ik_{4\mu'}\epsilon_{\nu'}^{(4)} - ik_{4\nu'}\epsilon_{\mu'}^{(4)})\epsilon^{(2)\mu'}\epsilon^{(0)\nu'} + (ik_{2\mu'}\epsilon_{\nu'}^{(2)} + ik_{2\nu'}\epsilon_{\mu'}^{(2)})\epsilon^{(0)\mu'}\epsilon^{(4)\nu'}\} \ . \quad (25)
\end{aligned}
$$

At this point we must recall that the three momenta of the external particles is small and neglected, so that we keep only spatial components of the polarization vectors. As a consequence, the term $(k_1 - k_3)^2$ in the ρ propagator is neglected. Similarly all terms of the type $k_{i\mu}\epsilon^\mu$, $k_{i\mu}\epsilon'^\mu$ can be neglected and only the terms $k_{i\mu}\epsilon^{(0)\mu}$ remain, since the exchanged vector can be time like (the only component that survives). As a consequence our amplitude gets much simplified and we obtain

$$
- it^{(ex)} = 2i\frac{g^2}{M_\rho^2}(k_1 \cdot k_4 + k_3 \cdot k_4 + k_1 \cdot k_2 + k_2 \cdot k_3)\epsilon_\mu \epsilon_\nu \epsilon^\mu \epsilon^\nu \ , \quad (26)
$$

with a unique spin structure, which can be recast, using momentum conservation into

$$
t^{(ex)} = -\frac{4g^2}{M_\rho^2}(\frac{3}{4}s - M_\rho^2)\epsilon_\mu \epsilon_\nu \epsilon^\mu \epsilon^\nu \ . \quad (27)
$$

The approximations done here are the same ones that one would do for the interaction of a vector with a pseudoscalar and which lead to the local chiral Lagrangian of [38, 21, 11] used to generate axial vector mesons in [21, 11]. This example serves to place our approximations in a due perspective, since such approximations are implicit in most of the effective chiral Lagrangians used in the literature [39], which can be deduced from the formalism of the hidden gauge Lagrangians that we are using here.

Before proceeding further one must evaluate the amplitudes for the different isospin states and we obtain

$$
t^{(ex,I=1)} = -\frac{2g^2}{M_\rho^2}(\frac{3}{4}s - M_\rho^2)(\epsilon_\mu \epsilon_\nu \epsilon^\mu \epsilon^\nu - \epsilon_\mu \epsilon_\nu \epsilon^\nu \epsilon^\mu) \ , \quad (28)
$$

which already projects over $S = 1$, as it should, such that

$$
t^{(ex,I=1,S=1)} = -4g^2(\frac{3s}{4M_\rho^2} - 1) \ . \quad (29)
$$

The case of $I = 0, 2$ is more subtle because, unlike the case of the contact term, we have now a t and u exchange channel, see fig. 7. When the two diagrams are considered we obtain

$$
t^{(ex,I=0)} = -\frac{4g^2}{M_\rho^2}(\frac{3}{4}s - M_\rho^2)(\epsilon_\mu \epsilon_\nu \epsilon^\mu \epsilon^\nu + \epsilon_\mu \epsilon_\nu \epsilon^\nu \epsilon^\mu) \ , \quad (30)
$$

which upon spin projection leads to

$$
\begin{aligned}
t^{(ex,I=0,S=0)} &= -8g^2(\frac{3s}{4M_\rho^2} - 1) \\
t^{(ex,I=0,S=2)} &= -8g^2(\frac{3s}{4M_\rho^2} - 1) \ . \quad (31)
\end{aligned}
$$

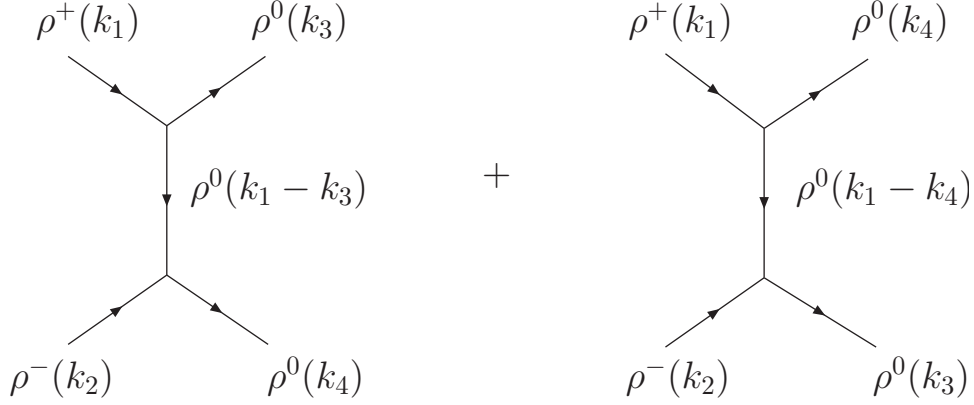Figure 7: t and u channel exchange of vector.

Similarly for $I = 2$ we obtain

$$t^{(ex,I=2)} = \frac{2g^2}{M_\rho^2}(\frac{3}{4}s - M_\rho^2)(\epsilon_\mu\epsilon_\nu\epsilon^\mu\epsilon^\nu + \epsilon_\mu\epsilon_\nu\epsilon^\nu\epsilon^\mu) \, , \tag{32}$$

which upon spin projection leads to

$$\begin{aligned}
t^{(ex,I=2,S=0)} &= 4g^2(\frac{3s}{4M_\rho^2} - 1) \\
t^{(ex,I=2,S=2)} &= 4g^2(\frac{3s}{4M_\rho^2} - 1) \, .
\end{aligned} \tag{33}$$

The results obtained with the contact term and the ρ-exchange mechanism provide the kernel, or potential V, to be used in the Bethe Salpeter equation in its on-shell factorized form,

$$T = \frac{V}{1 - VG} \, , \tag{34}$$

for each spin-isospin channel independently, where G is the two ρ loop function in the approximation of neglecting the on-shell three momenta

$$G = i \int \frac{d^4q}{(2\pi)^4} \frac{1}{q^2 - m_\rho^2 + i\epsilon} \frac{1}{(P-q)^2 - m_\rho^2 + i\epsilon} \, , \tag{35}$$

which upon using dimensional regularization can be recast as

$$\begin{aligned}
G &= \frac{1}{16\pi^2}\Big(\alpha + Log\frac{m_1^2}{\mu^2} + \frac{m_2^2 - m_1^2 + s}{2s}Log\frac{m_2^2}{m_1^2} \\
&+ \frac{p}{\sqrt{s}}\Big(Log\frac{s - m_2^2 + m_1^2 + 2p\sqrt{s}}{-s + m_2^2 - m_1^2 + 2p\sqrt{s}} + Log\frac{s + m_2^2 - m_1^2 + 2p\sqrt{s}}{-s - m_2^2 + m_1^2 + 2p\sqrt{s}}\Big)\Big) \, ,
\end{aligned} \tag{36}$$

where P is the total four-momentum of the two mesons, p is the three-momentum of the mesons in the center of mass frame and $m_1 = m_2 = m_\rho$, or using a cut off as

$$G = \int_0^{q_{max}} \frac{q^2 dq}{(2\pi)^2} \frac{\omega_1 + \omega_2}{\omega_1\omega_2[(P^0)^2 - (\omega_1 + \omega_2)^2 + i\epsilon]} \, , \tag{37}$$

11

where q_{max} stands for the cut off, $\omega_i = (\vec{q}_i^2 + m_i^2)^{1/2}$ and the center-of-mass energy $(P^0)^2 = s$. The potential V obtained summing the lowest order T matrices obtained from the contact term and ρ exchange are summarized in Table 1.

In Table 1 we have written in the last column the quantum numbers of the state and the

I	S	Contact	Exchange	$\sim Total[I^G(J^{PG})]$
1	1	$6g^2$	$-4g^2(\frac{3s}{4M_\rho^2} - 1)$	$-2g^2[1^+(1^{+-})]$
0	0	$8g^2$	$-8g^2(\frac{3s}{4M_\rho^2} - 1)$	$-8g^2[0^+(0^{++})]$
0	2	$-4g^2$	$-8g^2(\frac{3s}{4M_\rho^2} - 1)$	$-20g^2[0^+(2^{++})]$
2	0	$-4g^2$	$4g^2(\frac{3s}{4M_\rho^2} - 1)$	$4g^2[0^+(2^{++})]$
2	2	$2g^2$	$4g^2(\frac{3s}{4M_\rho^2} - 1)$	$10g^2[0^+(2^{++})]$

Table 1: V for the different spin isospin channels

approximate strength of the potential calculated at the $\rho\rho$ threshold to get an idea of the weight of the interaction. We observe attraction in the $I, S = 1, 1; 0, 0$ and $0, 2$ channels and repulsion in $2, 0; 2, 2$. We, thus, can not generate $I = 2$ low lying states from this $\rho\rho$ interaction. We find a weak attraction for the $I, S = 1, 1$ with $1^+(1^{+-})$ quantum numbers and then a strong attraction for $I, S = 0, 0$ and a much larger attraction for $I, S = 0, 2$, anticipating that if the interaction leads to a bound $\rho\rho$ state with $I, S = 0, 0$ it will necessarily lead to a much deeper bound $I, S = 0, 2$ state, a trend actually followed by the $f_0(1370)$ and $f_2(1270)$ resonances. The case of $I, S = 1, 1$ with $1^+(1^{+-})$ quantum numbers is special. These are the quantum numbers of the $b_1(1235)$. This state is generated dynamically from the interaction of vector mesons with pseudoscalars, the KK^* channel being the most important one [11]. The weak interaction of the possible $\rho\rho$ component of this state and the fact the $\rho\rho$ threshold is $300\,MeV$ above the mass of the $b_1(1235)$ anticipate that the $\rho\rho$ channel investigated here will have little effect modifying the results obtained for that resonance from the dynamics of the KK^* interaction. The weak attraction in this channel does not support a $\rho\rho$ bound state but could lead to a broad resonance at higher energies that we do not investigate here.

One may wonder about mixing the ω channel with the ρ. One can easily see that there are no contact terms with ω and the three vector vertices mixing ω with ρ are also forbidden since $\rho\omega\omega$ violates isospin and $\rho\rho\omega$ violates G parity.

The formalism that we are using is also allowed for s-channel ρ exchange and we can have the diagram of fig. 8. By performing similar approximations as done before we obtain an amplitude only in $I = 1, S = 0$ of the type

$$t^{(s)} = 24g^2 \frac{1}{(k_1 + k_2)^2 - M_\rho^2} \vec{k}_1 \cdot \vec{k}_3 , \qquad (38)$$

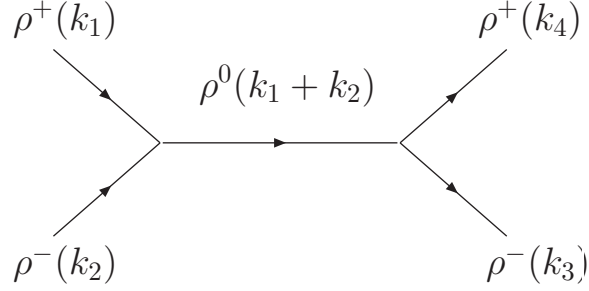which is a p-wave amplitude and repulsive. Note it also satisfies $L + S + I = even$.

Figure 8: S-channel ρ exchange diagram.

6   Convolution due to the ρ mass distribution

The strong attraction in the $I, S = 0, 0; 0, 2$ channels will produce $\rho\rho$ bound states and thus with no width within the model. However, this is not strictly true because the ρ has a large width or equivalently a mass distribution that allows the states obtained to decay in $\rho\rho$ for the low mass components of the ρ mass distribution. To take this into account we follow the traditional method which is to convolute the G function for the mass distributions of the two ρ mesons [40] replacing the G function by $\tilde{G}$ as follows

$$\tilde{G}(s) = \frac{1}{N^2} \int_{(m_\rho - 2\Gamma_\rho)^2}^{(m_\rho + 2\Gamma_\rho)^2} d\tilde{m}_1^2 (-\frac{1}{\pi}) \mathcal{I}m \frac{1}{\tilde{m}_1^2 - m_\rho^2 + i\Gamma\tilde{m}_1}$$
$$\times \int_{(m_\rho - 2\Gamma_\rho)^2}^{(m_\rho + 2\Gamma_\rho)^2} d\tilde{m}_2^2 (-\frac{1}{\pi}) \mathcal{I}m \frac{1}{\tilde{m}_2^2 - m_\rho^2 + i\Gamma\tilde{m}_2} G(s, \tilde{m}_1^2, \tilde{m}_2^2) , \qquad (39)$$

with

$$N = \int_{(m_\rho - 2\Gamma_\rho)^2}^{(m_\rho + 2\Gamma_\rho)^2} d\tilde{m}_1^2 (-\frac{1}{\pi}) \mathcal{I}m \frac{1}{\tilde{m}_1^2 - m_\rho^2 + i\Gamma\tilde{m}_1} , \qquad (40)$$

where $\Gamma_\rho = 146.2 \, MeV$ and for $\Gamma \equiv \Gamma(\tilde{m})$ we take the ρ width for the decay into the pions in p-wave

$$\Gamma(\tilde{m}) = \Gamma_\rho (\frac{\tilde{m}^2 - 4m_\pi^2}{m_\rho^2 - 4m_\pi^2})^{3/2} \theta(\tilde{m} - 2m_\pi) \qquad (41)$$

The use of $\tilde{G}$ in eq. (34) provides a width to the states obtained.

7   Results

In the first step we calculate the T matrix for the scattering of $\rho\rho$ in the two channels $I, S = 0, 0; 0, 2$ which experience the largest attraction according to Table 1. We consider the potential coming from the contact and exchange term, not the approximate sum shown in the table. For reasonable choices of the cut off, q_{max}, of the order of $1 \, GeV$ we always find bound states for both sets of quantum numbers, easily visible since T goes to infinity at values of $\sqrt{s}$ smaller than two ρ-meson masses. In Table 2 we show the energies of the bound states for different values of the cut off when we take a fixed ρ mass equal to its nominal mass.

I	S	$\sqrt{s}\,(MeV)[q_{max} = 875\,MeV/c]$	$\sqrt{s}\,(MeV)[q_{max} = 1000\,MeV/c]$
0	0	1512	1491
0	2	1255	1195

Table 2: Pole positions for the two different channels

We have used two values of the cut off around $1\,GeV/c$, $875\,MeV/c$ and $1000\,MeV/c$. What we see is that in both cases, and for higher values of q_{max}, one gets bound states for both $S = 0, S = 2$, and the binding of the $S = 2$ state is bigger than for $S = 0$. Since the strength of the potential for $S = 2$ is much bigger than for $S = 0$, we also see that the binding of the tensor state is more sensitive to the cut off than that of the scalar state. Yet, reasonable changes of q_{max} around $1\,GeV$ revert into changes of about $50\,MeV$ in the binding for the tensor state and about $20\,MeV$ for the scalar state. As usually done in this kind of calculations, once one shows the qualitative features of the states obtained, one can do some fine tuning of the parameters, only q_{max} in the present case, in order to match the energy of a certain state. In this case we choose the $f_2(1270)$ tensor state, since its mass is very precisely determined from different experiments [37] at $1275\,MeV$. Unlike the case of the $f_2(1270)$ state which has a well defined mass, the $f_0(1370)$ has a large dispersion of values in the PDG [37] to the point that they quote a mass $1200 - 1500\,MeV$ as their average.

As to the width, in our calculation it is obviously zero in both cases since we have obtained $\rho\rho$ bound states. Experimentally we have $\Gamma(f_2(1270)) = 184.4^{+3.9}_{-2.5}\,MeV$ and $\Gamma(f_0(1370)) = 200 - 500\,MeV$ according to [37]. Let us see if we can find a reasonable width for these states once we take into account the ρ mass distribution as described in the former section.

In fig. 9 we show the results for $|T|^2$ obtained by considering the ρ mass distribution. We show the results for the two cut offs of Table 2. As we can see in the figure, the matching of the mass of the $f_2(1270)$ is obtained with a cut off $q_{max} = 875\,MeV/c$. Then we obtain $1532\,MeV$ for the energy of the $S = 0$ state that we would like to associate to the $f_0(1370)$. Given, large dispersion of masses of the $f_0(1370)$, the results obtained by us would be consistent with the present experimental observation.

We see that $|T|^2$ has a good Breit Wigner distribution in both cases, with a peak around the masses shown in Table 2, but changed slightly. However, the widths are relatively small. For the tensor state one finds a width of about $2 - 3\,MeV$ and for the scalar state the width is about $50 - 75\,MeV$, depending on the cut off.

We see that the consideration of the ρ mass distribution leads indeed to a width of the states, but it is still very small compared with experiment, particularly for the tensor state. Clearly, there must be other sources of imaginary part. The likely candidate for the decay must be two pions, and indeed this accounts for 84.7% of the total width in the case of the $f_2(1270)$. The case of the $f_0(1370)$ is less clear since the two pion fraction can be of the order of 20% [37] while the 4π fraction could be dominant.

In the next section we address this problem and study the mechanisms that lead to the two pions decay of the two ρ system.
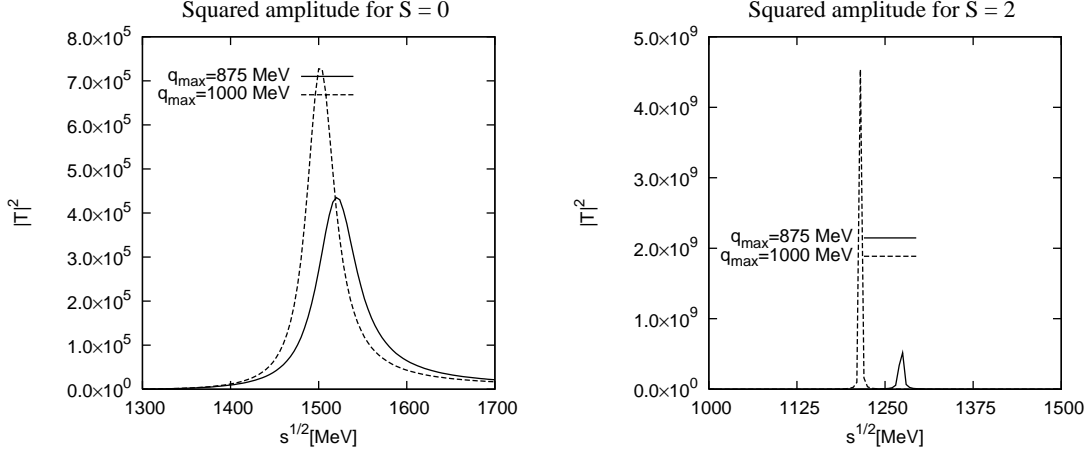
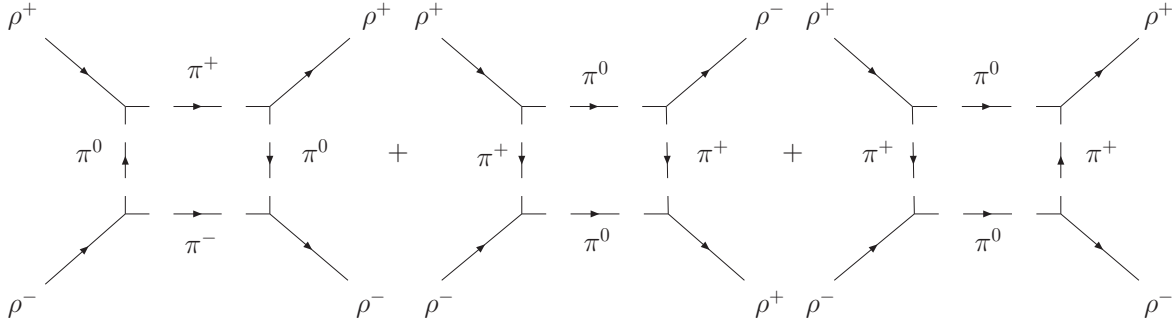Figure 9: $|T|^2$ taking into account the ρ mass distribution for $S = 0$ and $S = 2$.

Figure 10: Diagrams considered for $\rho\rho \to \pi\pi$.

8   Consideration of the two pion decay mode

The results obtained are interesting in as much as we are obtaining the two states $f_0(1370)$ and $f_2(1270)$ qualitatively, with the important fact that the $f_2(1270)$ state is more bound than the $f_0(1370)$. In this section we take into account the diagrams that couple $\rho\rho$ to $\pi\pi$, thus mixing the $\pi\pi$ channel with the $\rho\rho$ and allowing the states obtained to develop a width from decay into $\pi\pi$.

The $\pi\pi$ interaction at these energies away from $\pi\pi$ threshold, in $L = 0$ and $L = 2$ that we will need for states of $J = 0, 2$ respectively, is rather weak compared with the one of the $\rho\rho$ interaction. Furthermore, the energies of the two resonances under discussion are close to the two ρ meson threshold and far away for that of $\pi\pi$. Hence, this latter channel cannot have much weight in the wave function of these resonances. It is, thus, unnecessary to treat the $\pi\pi$ as a coupled channel and one can simplify the work by computing the diagrams for $\rho\rho \to \rho\rho$ mediated by two pion exchange depicted in fig. 10 for $\rho^+\rho^- \to \rho^+\rho^-$. If we introduce these new terms
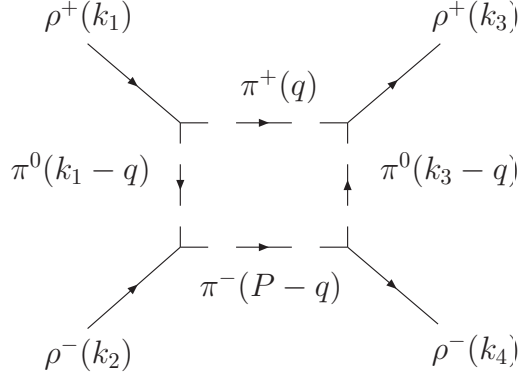
15

Figure 11: Detail of one of the diagrams of fig. 10.

as part of the $\rho\rho$ interaction and iterate them through the Bethe Salpeter equation of eq. (34), we generate all terms with transition of $\rho\rho$ to $\pi\pi$ and neglect terms containing the $\pi\pi \to \pi\pi$ interaction that we considered weaker.

The evaluation of the box diagram in fig. 11, where the momenta are explicitly shown, is straightforward. One needs the $\rho\pi\pi$ couplings which are provided within the same framework of the hidden gauge formalism [22, 23] by means of the Lagrangian

$$\mathcal{L}_{V\Phi\Phi} = -ig\langle V^\mu[\Phi, \partial_\mu\Phi]\rangle . \tag{42}$$

We have:

$$
\begin{aligned}
- it^{(\pi\pi)} &= \int \frac{d^4q}{(2\pi)^4}(-i)(\sqrt{2}g)^4(q - k_1 + q)^\mu \epsilon_\mu^{(1)} \\
&\times \ i(k_1 - q + P - q)_\nu \epsilon^{(2)\nu} i(k_3 - q - q)_\alpha \epsilon^{(3)\alpha}(-i)(q - k_3 - P + q)_\beta \epsilon^{(4)\beta} \\
&\times \ \frac{i}{q^2 - m_\pi^2 + i\epsilon} \frac{i}{(k_1 - q)^2 - m_\pi^2 + i\epsilon} \\
&\times \ \frac{i}{(P - q)^2 - m_\pi^2 + i\epsilon} \frac{i}{(k_3 - q)^2 - m_\pi^2 + i\epsilon} .
\end{aligned}
\tag{43}
$$

By making again the approximation that all the polarization vectors are spatial, we can rewrite the amplitude as

$$
\begin{aligned}
- it^{(\pi\pi)} &= (\sqrt{2}g)^4 \int \frac{d^4q}{(2\pi)^4} 16 \, q_i q_j q_l q_m \, \epsilon_i^{(1)} \epsilon_j^{(2)} \epsilon_l^{(3)} \epsilon_m^{(4)} \\
&\times \ \frac{1}{q^2 - m_\pi^2 + i\epsilon} \frac{1}{(k_1 - q)^2 - m_\pi^2 + i\epsilon} \\
&\times \ \frac{1}{(P - q)^2 - m_\pi^2 + i\epsilon} \frac{1}{(k_3 - q)^2 - m_\pi^2 + i\epsilon} .
\end{aligned}
\tag{44}
$$

Since the integral is logarithmically divergent, and in the absence of data to fit the subtraction constant if using dimensional regularization, we regularize it with a cut off in the three momentum, which should be of the order of $1\,GeV$, the basic scale at the energies that we are working. This

16

requires to perform the q^0 integration analytically, which is easily done by means of the residues, caring to divide exactly by factors with undefined polarity ($\pm i\epsilon$ in factors of the denominator). The procedure proves more practical in this case than using the Feynman parametrization, which requires three integrals, while here we need only one. Furthermore, the cuts, or sources of imaginary part show up explicitly and allow one to keep control in the numerical evaluation. After some algebraic manipulation we obtain

$$
\begin{aligned}
V^{(\pi\pi)} &= (\sqrt{2}g)^4 \left(\epsilon_i^{(1)} \epsilon_i^{(2)} \epsilon_j^{(3)} \epsilon_j^{(4)} + \epsilon_i^{(1)} \epsilon_j^{(2)} \epsilon_i^{(3)} \epsilon_j^{(4)} + \epsilon_i^{(1)} \epsilon_j^{(2)} \epsilon_j^{(3)} \epsilon_i^{(4)} \right) \\
&\times \quad \frac{8}{15\pi^2} \int_0^{q_{max}} dq\, \vec{q}^{\,6} \left\{ 10\omega^2 - (k_3^0)^2 \right\} \frac{1}{\omega^3} \left(\frac{1}{k_1^0 + 2\omega} \right)^2 \frac{1}{P^0 + 2\omega} \\
&\times \quad \frac{1}{k_1^0 + \frac{\Gamma}{4} - 2\omega + i\epsilon} \frac{1}{k_1^0 - \frac{\Gamma}{4} - 2\omega + i\epsilon} \frac{1}{P^0 - 2\omega + i\epsilon} ,
\end{aligned}
\tag{45}
$$

with $\omega = \sqrt{\vec{q}^{\,2} + m_\pi^2}$. We see the two sources of imaginary part in the cuts $k_1^0 \pm \frac{\Gamma}{4} - 2\omega = 0$ and $P^0 - 2\omega = 0$, corresponding to $\rho \to \pi\pi$ and $\rho\rho \to \pi\pi$. The diagram of Fig. 11 leads to a double pole for $\rho \to \pi\pi$, a decay channel that is open at the energies that we study . But when the mass distribution of the ρ is considered in the evaluation of the amplitude, the degeneracy of the pole is removed. We have performed such a calculation, but have observed that a simpler approach, and accurate enough for our purposes, is to substitute the double pole $(1/(k_1^0 - 2\omega + i\epsilon))^2$, which appears in the calculation with fixed ρ masses, by $(1/(k_1^0 - 2\omega + \frac{\Gamma}{4} + i\epsilon)) (1/(k_1^0 - 2\omega - \frac{\Gamma}{4} + i\epsilon))$ to approximatly account for the dispersion of ρ masses in the convolution. We see in practice that the results barely change if we put there $\Gamma/2$ instead of $\Gamma/4$ or some other reasonable number of the size of the ρ width.

The spin structure projects over $S = 0, S = 2$, not over $S = 1$, which is obvious since the parity of the $\rho\rho$ system for ρ in s-wave is positive which forces the two pions in $L = 0, 2$, equivalent to total J since the pions have no spin. Hence we find only the $0^+, 2^+$ quantum numbers.

The next step is to evaluate the diagrams shown in Fig. 10 for $\rho^+\rho^- \to \rho^+\rho^-$ in the case of $\rho^+\rho^- \to \rho^0\rho^0$, etc, to obtain the isospin combinations. We are only interested in $I = 0$, for the two states found in the former sections. So we obtain finally

$$
\begin{aligned}
t^{(2\pi,I=0,S=0)} &= 20\, \tilde{V}^{(\pi\pi)} \\
t^{(2\pi,I=0,S=2)} &= 8\, \tilde{V}^{(\pi\pi)}
\end{aligned}
\tag{46}
$$

where $\tilde{V}^{(\pi\pi)}$ is given by the eq. (45) after removing the polarization vectors.

The integral of eq. (45) is logarithmically divergent, a divergence that can be smoothly regularized with a cut off as we have done before. We have checked that with the former cut off the real part obtained from $V^{(\pi\pi)}$ is fairly smaller than that obtained from the $\rho\rho$ potentials of Table 1. On the other hand, there is also another source of real part from the box diagram involving the $\rho\omega\pi$ anomalous coupling, which has a similar structure ($\vec{q}^{\,6}$ factor in the integrand), and is also smaller than the potentials of Table 1 and of opposite sign to $V^{(\pi\pi)}$. Altogether, we neglect the real parts of these box diagrams and take the real part of the potential from the tree level potential of Table 1. In the next section we come back to these issues with a detailed evaluation. However, $V^{(\pi\pi)}$ leads now to a large imaginary part of the resonances because of the large phase space for $\pi\pi$ decay. The largest piece of the imaginary part comes from the factor $(P^0 - 2\omega + i\epsilon)^{-1}$. Since we are concerned about the width of the resonances, we, thus, consider
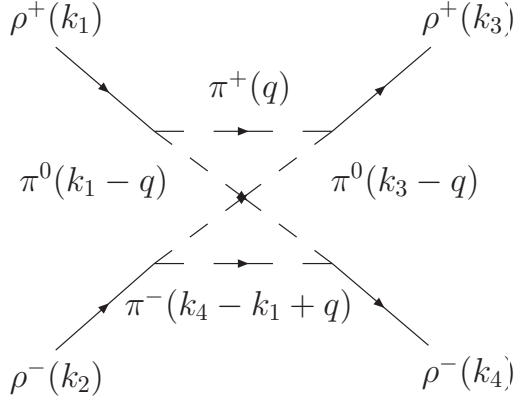
Figure 12: Crossed-box diagram for the four pion decay mode.

the π exchange between two ρ mesons in the t channel as mostly off shell and implement empirical form factors used in the decay of vector mesons in [41],[42]. We use

$$F(q) = \frac{\Lambda^2 - m_\pi^2}{\Lambda^2 - (k-q)^2} \tag{47}$$

in each $\rho \to \pi\pi$ vertex with

$$k^0 = \frac{\sqrt{s}}{2} \quad \vec{k} = 0 \quad q^0 = \frac{\sqrt{s}}{2} , \tag{48}$$

and $\vec{q}$ the running variable in the integral.

We shall evaluate the results for different values of Λ around $1200 - 1300\,MeV$, which are the values chosen in [41],[42]. We also implement a global cut off of $q_{max} = 1.2\,GeV$ in the integral of eq. (45), although the form factors already provide fast convergence around that region.

9 Consideration of the crossed-$\pi\pi$ box diagrams and the two omega intermediate state

We can also have the crossed diagram of Fig. 12. By following identical steps as for the diagram of Fig. 11 we obtain at the end the expression

$$
\begin{aligned}
\tilde{V}^{(c,\pi\pi)} &= \frac{16\,g^4}{15\pi^2} \int_0^{q_{max}} dq\, \vec{q}^{\,6} \{20\omega^2 - (k_1^0)^2\} \frac{1}{\omega^3} \left(\frac{1}{k_1^0 + 2\omega}\right)^3 \\
&\times \frac{1}{k_1^0 + \frac{\Gamma}{4} - 2\omega + i\epsilon} \frac{1}{k_1^0 - \frac{\Gamma}{4} - 2\omega + i\epsilon} \frac{1}{k_1^0 - 2\omega + i\epsilon}
\end{aligned}
\tag{49}
$$

and

$$
\begin{aligned}
t^{(2\pi(c),I=0,S=0)} &= 5\,\tilde{V}^{(c,\pi\pi)} \\
t^{(2\pi(c),I=0,S=2)} &= 2\,\tilde{V}^{(c,\pi\pi)} .
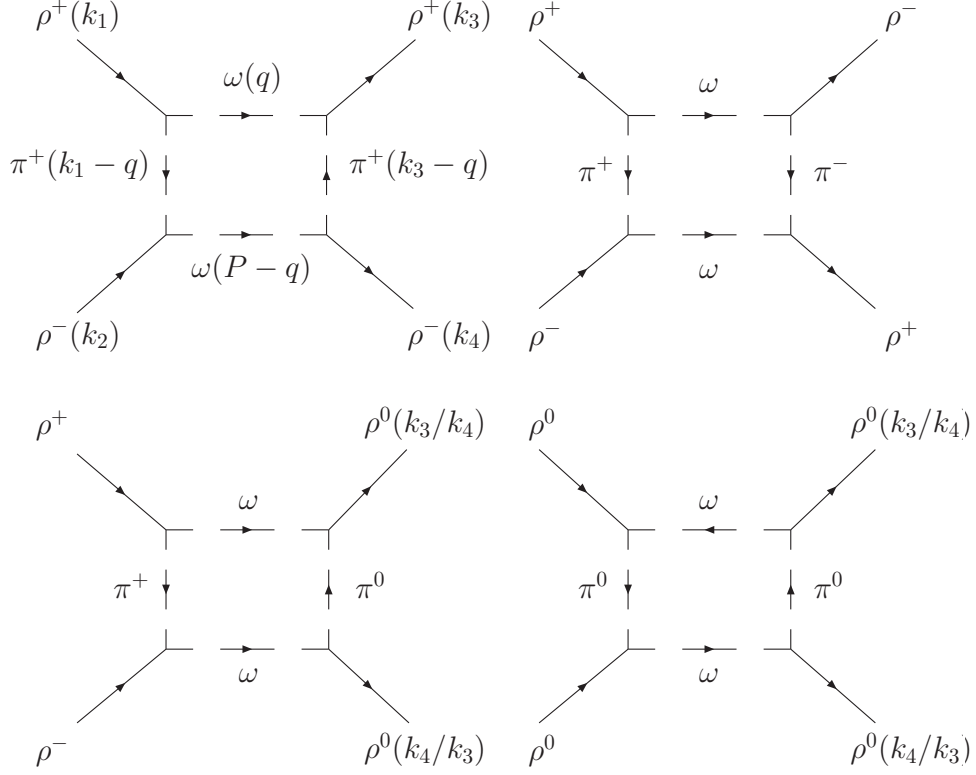\end{aligned}
\tag{50}
$$

18

Figure 13: Anomalous-box diagrams for the two omega intermediate state.

It is also interesting to evaluate the contribution of intermediate $\omega\omega$ state with anomaluous couplings, given by Fig. 13. The coupling $\rho\omega\pi$, with the renormalization that we use, can be found in [33] and is given by

$$\mathcal{L}_{VVP} = \frac{G'}{\sqrt{2}}\epsilon^{\mu\nu\alpha\beta}\langle\partial_\mu V_\nu \partial_\alpha V_\beta\, P\rangle \tag{51}$$

with

$$G' = \frac{3g'^2}{4\pi^2 f} \qquad g' = -\frac{G_V M_\rho}{\sqrt{2}f^2}\ ,$$

where $G_V \simeq 55\,MeV$ and $f_\pi = 93\,MeV$. Thus, the vertex $\rho^+\pi^+\omega$ give

$$-it = iG'\epsilon^{\mu\nu\alpha\beta}\, q_\mu\, k_{1,\alpha}\, \epsilon_\nu(\omega)\, \epsilon_\beta(\rho^+)\ . \tag{52}$$

At this point we use again the assumption that $\vec{k}_{i,j} \simeq 0$ which forces the index $\alpha = 0$, and one obtain

$$-it = iG' M_\rho\, \epsilon_{ijk}\, q_i\, \epsilon_j(\omega)\, \epsilon_k(\rho^+)\ . \tag{53}$$

The amplitude corresponding to the first diagram of Fig. 13 is given by

$$-it^{(\omega\omega)} = \int \frac{d^4q}{(2\pi)^4}\, M_\rho^4\, G'^4\, \epsilon_{i_1 j_1 k_1}\, q_{i_1}\, \epsilon_{j_1}(\omega)\, \epsilon_{k_1}(\rho_1^+)\, \epsilon_{i_2 j_2 k_2}\, q_{i_2}\, \epsilon_{j_2}(\omega)\, \epsilon_{k_2}(\rho_2^-)$$

19

$$\times \quad \epsilon_{i_3 j_3 k_3} q_{i_3} \, \epsilon_{j_3}(\omega) \, \epsilon_{k_3}(\rho_4^-) \; \epsilon_{i_4 j_4 k_4} \, q_{i_4} \, \epsilon_{j_4}(\omega) \, \epsilon_{k_4}(\rho_3^+) \; \frac{1}{q^2 - M_\omega^2 + i\epsilon}$$

$$\times \quad \frac{1}{(P-q)^2 - M_\omega^2 + i\epsilon} \; \frac{1}{(k_1 - q)^2 - m_\pi^2 + i\epsilon} \; \frac{1}{(k_3 - q)^2 - m_\pi^2 + i\epsilon} \;, \tag{54}$$

which upon sum over the internal ω polarizations and simplifications done before, leads to

$$
\begin{aligned}
t^{(\omega\omega)} \;=\;& -f(\epsilon_i) \frac{1}{15} M_\rho^4 \, G'^4 \int \frac{d^3 q}{(2\pi)^3} \, \vec{q}^{\,4} \left(-\omega_\pi^3 + k_3^{0\,2}\omega_\omega - 4\,\omega_\pi^2\omega_\omega - 4\,\omega_\pi\omega_\omega^2 - \omega_\omega^3 \right) \\
& \times \quad \frac{1}{(k_1^0 + \omega_\omega + \omega_\pi)^2} \; \frac{1}{(\omega_\omega + \omega_\pi - k_1^0 - i\epsilon)} \; \frac{1}{(\omega_\omega + \omega_\pi - k_3^0 - i\epsilon)} \\
& \times \quad \frac{1}{\omega_\pi^3} \frac{1}{(P^0 - 2\omega_\omega + i\epsilon)} \frac{1}{(P^0 + 2\omega_\omega)} \frac{1}{\omega_\omega} \;,
\end{aligned}
\tag{55}
$$

where $f(\epsilon_i) = 6\,(\vec{\epsilon}_1 \cdot \vec{\epsilon}_3)(\vec{\epsilon}_2 \cdot \vec{\epsilon}_4) + (\vec{\epsilon}_1 \cdot \vec{\epsilon}_2)(\vec{\epsilon}_3 \cdot \vec{\epsilon}_4) + (\vec{\epsilon}_1 \cdot \vec{\epsilon}_4)(\vec{\epsilon}_2 \cdot \vec{\epsilon}_3)$. When we evaluate the $\rho\rho$ interaction in $I = 0$, the only one in this case, $f(\epsilon_i)$ is changed to

$$f"(\epsilon_i) = 7\,(\vec{\epsilon}_1 \cdot \vec{\epsilon}_3)(\vec{\epsilon}_2 \cdot \vec{\epsilon}_4) + 7\,(\vec{\epsilon}_1 \cdot \vec{\epsilon}_4)(\vec{\epsilon}_2 \cdot \vec{\epsilon}_3) + 2(\vec{\epsilon}_1 \cdot \vec{\epsilon}_2)(\vec{\epsilon}_3 \cdot \vec{\epsilon}_4) \;, \tag{56}$$

which allows the projection over $S = 0$ and $S = 2$, and we finally obtain

$$
\begin{aligned}
\tilde{V}^{(\omega\omega)} \;=\;& -\frac{1}{30\,\pi^2} M_\rho^4 \, G'^4 \int_0^{q_{max}} dq \, \vec{q}^{\,4} \left(-\omega_\pi^3 + k_3^{0\,2}\omega_\omega - 4\,\omega_\pi^2\omega_\omega - 4\,\omega_\pi\omega_\omega^2 - \omega_\omega^3 \right) \\
& \times \quad \frac{1}{(k_1^0 + \omega_\omega + \omega_\pi)^2} \; \frac{1}{(k_1^0 + \frac{\Gamma}{4} - \omega_\omega - \omega_\pi + i\epsilon)} \; \frac{1}{(k_3^0 - \frac{\Gamma}{4} - \omega_\omega - \omega_\pi + i\epsilon)} \\
& \times \quad \frac{1}{\omega_\pi^3} \frac{1}{(P^0 - 2\omega_\omega + i\epsilon)} \frac{1}{(P^0 + 2\omega_\omega)} \frac{1}{\omega_\omega}
\end{aligned}
\tag{57}
$$

and

$$
\begin{aligned}
t^{(\omega\omega, I=0, S=0)} \;&=\; 30\,\tilde{V}^{(\omega\omega)} \\
t^{(\omega\omega, I=0, S=2)} \;&=\; 21\,\tilde{V}^{(\omega\omega)} \;.
\end{aligned}
\tag{58}
$$

In Fig. 14 we show the different contributions to the potential that we have considered for $I = 0$, $S = 0$ and $I = 0$, $S = 2$. In the evaluation of the integrals we have taken the same cut off of $q_{max} = 1200\,MeV$. For the sake of simplicity, the calculations are done without form factors. Their consideration does not change the conclusions that follow. Concerning the real parts, in the case of $S = 2$ we observe that the most important contribution is the potential coming from the contact term and the ρ-exchange, which is very large and attractive, whereas the other terms are practically zero. For $S = 0$ we observe that the individual contributions of the $\pi\pi$-box diagram, crossed-$\pi\pi$-box diagram and $\omega\omega$ term are comparatively larger with respect to the contact plus ρ-exchange term than in the case of $S = 2$. Yet, we find a quite good cancellation of the $\pi\pi$ box plus crossed-$\pi\pi$ box and anomalous-$\omega\omega$ box terms, and the interaction is dominated by the contact plus ρ-exchange terms. However, the relatively larger contribution of the subdominant terms indicates that we should admit larger uncertainties in the position of the $f_0(1370)$ state than in the $f_2(1270)$ one. For the imaginary parts we see that the term of the $\pi\pi$ box, which allows for the decay of $\rho\rho$ in $\pi\pi$, is considerably larger than the others, and we obtain that the
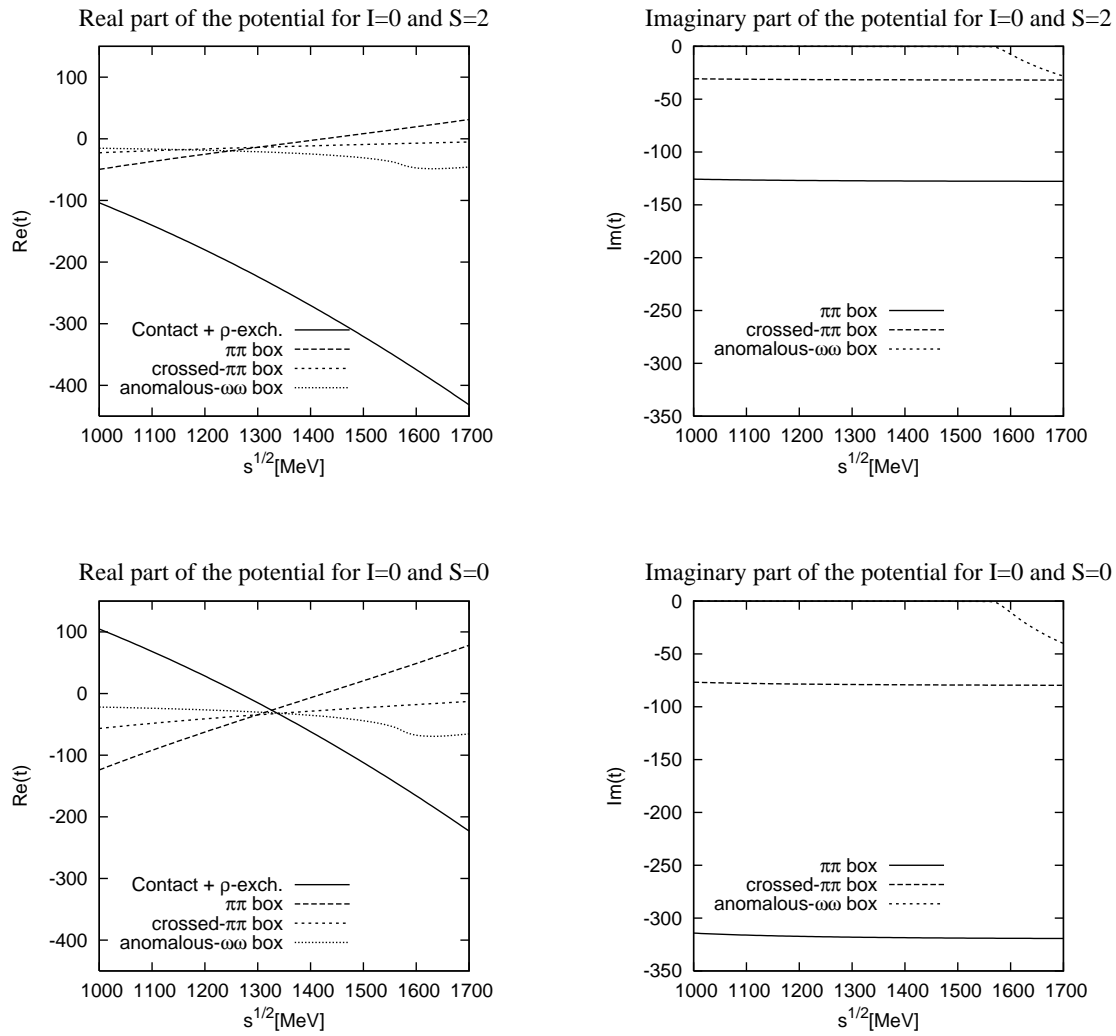
Figure 14: Comparison of the real and imaginary parts of the different potentials for $I = 0$, $S = 2$ and $I = 0$, $S = 0$.

crossed-$\pi\pi$ box (decay in 4π) only accounts for the 20% of the $\pi\pi$ box, whereas the anomalous-$\omega\omega$ box is zero in our region of interest.

As we see, the crossed terms are reasonably smaller than the direct ones. We use this fact to omit the calculation of the crossed pion terms corresponding to the convolution of the two $\rho's$. This convolution implicitly includes the contribution of four intermediate pions when the two meson decay each into two pions. We could make one of two pions from one ρ to be reabsorbed by the other ρ. We saw that the convolution of the $\rho's$ gave rise to a moderate width compared with the direct $\pi\pi$ box. Since the crossed-$\pi\pi$ box gives a smaller contribution than the direct term, we can expect the same to occur with the crossed terms from the convolution, giving rise to a small correction to a width which is already much smaller than the one obtained from the 2π decay. For this reason we omit the evaluation of these terms.

10   Results with $V^{(\pi\pi)}$

In view of the results obtained in the former section, here we show the results obtained considering only the contact term plus the ρ-exchange term and the imaginary part of the direct $\pi\pi$-box diagram. The 20% extra contribution to the imaginary part of the $\pi\pi$-crossed box term is small compared with uncertainties in the width stemming from the use of the form factor of eq. (47).

In fig. 15 we show the results for $|T|^2$ including the $\pi\pi$ box mechanism for a chosen value of $\Lambda = 1300\,MeV$ and the two values of the cut off. What we observe is that the peak positions are barely changed with respect to fig. 9, however, the widths are now considerably larger. For the case of the $S = 0$ state the width is of the order of $\Gamma = 200\,MeV$, while for the case of the $S = 2$ state is of the order of $110\,MeV$. The experimental situation is the following. The $f_2(1270)$ has a width of $\Gamma = 185\,MeV$ mostly (85%) coming from $\pi\pi$ decay [37]. This means $\Gamma_{\pi\pi} \simeq 156\,MeV$, which should be considered in fair agreement with our results. For the case of the $f_0(1370)$ the width is $200-500\,MeV$ according to the PDG [37], with about 50% of the experiments providing a width around $200\,MeV$ in agreement with our findings. One might wonder whether the scalar state that we obtain, which has a mass around $1500\,MeV$, could not correspond to the $f_0(1500)$. However, its width of about $100\,MeV$, out of which only 35% comes from $\pi\pi$ decay [37], clearly excludes it from being associated to the state that we have obtained around $1500\,MeV$. On the other hand, preliminary data from the Belle collaboration suggest that the peak of the mass of the $f_0(1370)$ appears rather around $1470\,MeV$ [43], which would agree better with our findings. Yet, one should also take into consideration the thorough study of [44], making a strong claim in favor of the $f_0(1370)$ with a mass around the nominal one of the PDG. Incidentally, this latter analysis relies upon a dispersive term dominated by $\rho\rho$ components.

Our model provides some 4π decay coming from the $\pi\pi$ decay of each ρ, which has been taken into account by means of the convolution with the ρ mass distribution. Also the crossed-$\pi\pi$ box diagram discussed in Section 9 gives rise to 4π decay. However, this cannot be the sole contribution of 4π decay. In a recent paper [45], extra decay channels of the type of $\sigma\sigma$ are also considered which would increase the total width.[2]

In order to show the sensitivity of the results to the meson decay form factor we show in

---

[2]This work is being further extended and a more detailed discussion at this point is untimely, but one should keep track of further developments along this line to implement further improvements in our approach.
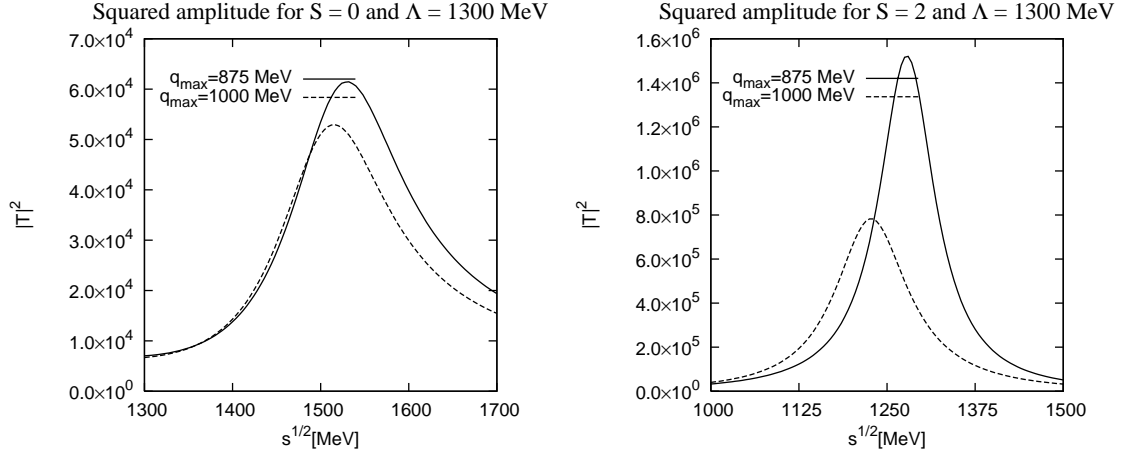
Figure 15: $|T|^2$ taking into account the $\pi\pi$ box with $\Lambda = 1300\,MeV$, $q_{max} = 875, 1000\,MeV$ for $S = 0$ and $S = 2$.

fig. 16 the results for different values of Λ, in the range of values used in [41],[42]. We take $\Lambda = 1200, 1300$ and $1400\,MeV$. We can see that as Λ grows, the width becomes larger but the peak position does not change. The dispersion on the values of the width gives us an indication of the theoretical uncertainties in this value. Yet, within these uncertainties in the position and the width, one can claim a reasonable agreement with data for these two states providing a big support for the idea of the two states as being dynamically generated from the $\rho\rho$ interaction given by the hidden gauge formalism.

11   Conclusions

We have made a study of the $\rho\rho$ interaction using the hidden gauge formalism. The interaction comes from contact terms plus ρ meson exchange in the t-channel. Amongst all spin and isospin allowed channels in s-wave, we found strong attraction, enough to bind the system, in $I = 0, S = 0$ and $I = 0, S = 2$. We also found that in the case of $I = 0, S = 2$ the interaction was more attractive, leading to a tensor state more bound than the scalar. The consideration of the ρ mass distribution gives a width to the two states, very small in the case of the tensor state because of its large binding. However, the biggest source of width comes from the decay into $\pi\pi$ that we have also studied within the same formalism. We found the width much larger for the case of the scalar state. We also studied the effect of the crossed-$\pi\pi$-box diagrams and the contribution of $\omega\omega$-intermediate states with anomalous couplings, which were found to play a minor role. The states obtained could be associated with the $f_0(1370)$ and $f_2(1270)$, for which we found a qualitative agreement on the mass and width. The findings of the paper give support to the idea that these two resonances are dynamically generated from the $\rho\rho$ interaction, or in other words, that they qualify largely as $\rho\rho$ molecules.
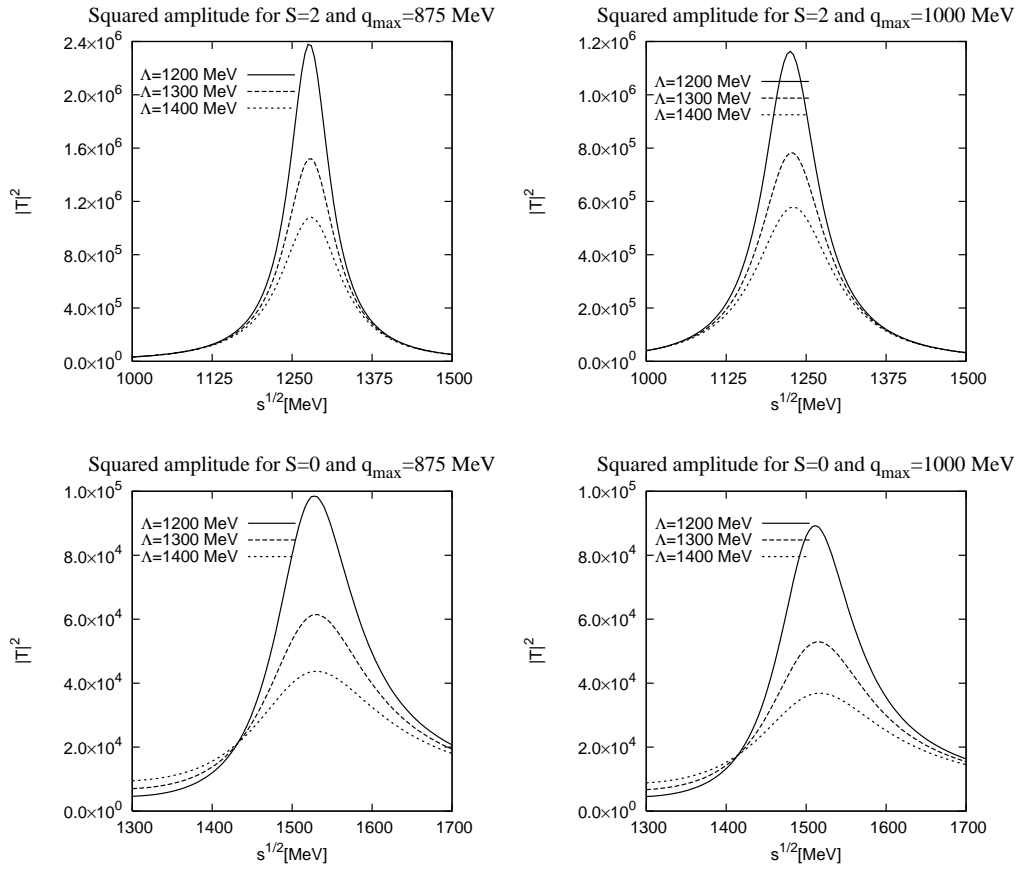
Figure 16: $|T|^2$ taking into account the $\pi\pi$ box for different values of $\Lambda = 1200, 1300, 1400\ MeV$ and $q_{max} = 875, 1000\ MeV$ for $S = 0$ and $S = 2$

Acknowledgments

References

[1] J. A. Oller and E. Oset, Phys. Rev. D **60**, 074023 (1999) [arXiv:hep-ph/9809337].

[2] J. A. Oller and U. G. Meissner, Phys. Lett. B **500**, 263 (2001) [arXiv:hep-ph/0011146].

[3] A. Dobado and J. R. Pelaez, Phys. Rev. D **56**, 3057 (1997) [arXiv:hep-ph/9604416].

[4] J. A. Oller, E. Oset and J. R. Pelaez, Phys. Rev. D **59**, 074001 (1999) [Erratum-ibid. D **60**, 099906 (1999)] .

[5] N. Kaiser, P. B. Siegel and W. Weise, Nucl. Phys. A **594**, 325 (1995) [arXiv:nucl-th/9505043].

[6] J. A. Oller and E. Oset, Nucl. Phys. A **620**, 438 (1997) [Erratum-ibid. A **652**, 407 (1999)] [arXiv:hep-ph/9702314].

[7] N. Kaiser, Eur. Phys. J. A **3**, 307 (1998).

[8] J. A. Oller, E. Oset and A. Ramos, Prog. Part. Nucl. Phys. **45**, 157 (2000) [arXiv:hep-ph/0002193].

[9] E. Oset *et al.*, arXiv:0806.0340 [nucl-th].

[10] D. Jido, J. A. Oller, E. Oset, A. Ramos and U. G. Meissner, Nucl. Phys. A **725**, 181 (2003) [arXiv:nucl-th/0303062].

[11] L. Roca, E. Oset and J. Singh, Phys. Rev. D **72**, 014002 (2005) [arXiv:hep-ph/0503273].

[12] V. K. Magas, E. Oset and A. Ramos, Phys. Rev. Lett. **95**, 052301 (2005) [arXiv:hep-ph/0503043].

[13] L. S. Geng, E. Oset, L. Roca and J. A. Oller, Phys. Rev. D **75**, 014017 (2007) [arXiv:hep-ph/0610217].

[14] V. E. Markushin, Eur. Phys. J. A **8**, 389 (2000) [arXiv:hep-ph/0005164].

[15] E. Oset and A. Ramos, Nucl. Phys. A **635** (1998) 99 .

[16] C. Garcia-Recio, M. F. M. Lutz and J. Nieves, Phys. Lett. B **582** (2004) 49 .

[17] C. Garcia-Recio, J. Nieves and L. L. Salcedo, Phys. Rev. D **74** (2006) 034025 .

[18] T. Hyodo, S. I. Nam, D. Jido and A. Hosaka, Phys. Rev. C **68**, 018201 (2003) [arXiv:nucl-th/0212026].

[19] E. E. Kolomeitsev and M. F. M. Lutz, Phys. Lett. B **585** (2004) 243 .

[20] S. Sarkar, E. Oset and M. J. Vicente Vacas, Nucl. Phys. A **750** (2005) 294 [Erratum-ibid. A **780** (2006) 78] .

[21] M. F. M. Lutz and E. E. Kolomeitsev, Nucl. Phys. A **730** (2004) 392 .

[22] M. Bando, T. Kugo, S. Uehara, K. Yamawaki and T. Yanagida, Phys. Rev. Lett. **54**, 1215 (1985).

[23] M. Bando, T. Kugo and K. Yamawaki, Phys. Rept. **164**, 217 (1988).

[24] A. Dobado and J. R. Pelaez, Phys. Rev. D **65**, 077502 (2002) [arXiv:hep-ph/0111140].

[25] A. H. Fariborz, Phys. Rev. D **74**, 054030 (2006) [arXiv:hep-ph/0607105].

[26] T. Umekawa, K. Naito, M. Oka and M. Takizawa, Phys. Rev. C **70**, 055205 (2004) [arXiv:hep-ph/0403032].

[27] S. Rodriguez and M. Napsuciale, Phys. Rev. D **71**, 074008 (2005) [arXiv:hep-ph/0411150].

[28] F. E. Close, Nucl. Phys. Proc. Suppl. **56A**, 248 (1997) [arXiv:hep-ph/9610426].

[29] F. Kleefeld, E. van Beveren, G. Rupp and M. D. Scadron, Phys. Rev. D **66**, 034007 (2002) [arXiv:hep-ph/0109158].

[30] A. V. Anisovich, V. V. Anisovich and V. A. Nikonov, Eur. Phys. J. A **12**, 103 (2001) [arXiv:hep-ph/0108186].

[31] J. Gasser and H. Leutwyler, Nucl. Phys. B **250**, 465 (1985).

[32] J. R. Pelaez, Phys. Rev. Lett. **92** (2004) 102001 [arXiv:hep-ph/0309292].

[33] H. Nagahiro, L. Roca, A. Hosaka and E. Oset, arXiv:0809.0943v1 [hep-ph]

[34] Riazuddin and Fayyazuddin, Phys. Rev. **147**, 1071 (1966).

[35] J.J. Sakurai, Currents and mesons (University of Chicago Press, Chicago Il 1969)

[36] L. Alvarez-Ruso and V. Koch, Phys. Rev. C **65**, 054901 (2002) [arXiv:nucl-th/0201011].

[37] W. M. Yao *et al.* [Particle Data Group], J. Phys. G **33**, 1 (2006).

[38] M. C. Birse, Z. Phys. A **355**, 231 (1996) [arXiv:hep-ph/9603251].

[39] U. G. Meissner, Rept. Prog. Phys. **56**, 903 (1993) .

[40] H. Nagahiro, L. Roca and E. Oset, Eur. Phys. J. A **36**, 73 (2008) [arXiv:0802.0455 [hep-ph]].

[41] A. I. Titov, B. Kampfer and B. L. Reznik, Eur. Phys. J. A **7**, 543 (2000)

[42] A. I. Titov, B. Kampfer and B. L. Reznik, Phys. Rev. C **65**, 065202 (2002)

[43] S. Uehara, private communication.

[44] D. V. Bugg, Eur. Phys. J. C **52**, 55 (2007) [arXiv:0706.1341 [hep-ex]].

[45] M. Albaladejo and J. A. Oller, arXiv:0801.4929 [hep-ph].